

CatchPhrase: EXPrompt-Guided Encoder Adaptation for Audio-to-Image Generation

Hyunwoo Oh
komjii@hanyang.ac.kr
Hanyang University
Seoul, Republic of Korea

SeungJu Cha
sju9020@hanyang.ac.kr
Hanyang University
Seoul, Republic of Korea

Kwanyoung Lee
mobled37@hanyang.ac.kr
Hanyang University
Seoul, Republic of Korea

Si-Woo Kim
boreng0817@hanyang.ac.kr
Hanyang University
Seoul, Republic of Korea

Dong-Jin Kim*
djdkim@hanyang.ac.kr
Hanyang University
Seoul, Republic of Korea

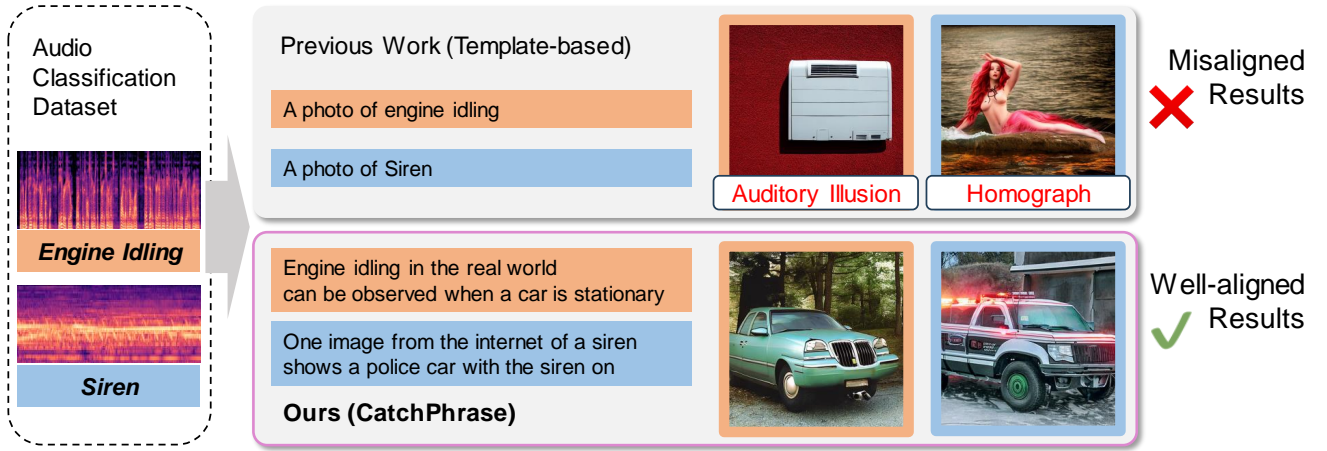


Figure 1: Visual demonstration of CatchPhrase. Unlike prior method [35] relying on fixed templates for audio-text alignment, CatchPhrase uses semantically enriched prompts from audio and text cues, producing well-aligned results for each audio sample.

Abstract

We propose **CatchPhrase**, a novel audio-to-image generation framework designed to mitigate semantic misalignment between audio inputs and generated images. While recent advances in multi-modal encoders have enabled progress in cross-modal generation, ambiguity stemming from *homographs* and *auditory illusions* continues to hinder accurate alignment. To address this issue, CatchPhrase generates enriched cross-modal semantic prompts (**EXPrompt Mining**) from weak class labels by leveraging large language models (LLMs) and audio captioning models (ACMs). To address both class-level and instance-level misalignment, we apply multi-modal filtering and retrieval to select the most semantically aligned prompt for each audio sample (**EXPrompt Selector**). A lightweight mapping network is then trained to adapt pre-trained text-to-image generation models to audio input. Extensive experiments on multiple audio classification datasets demonstrate that CatchPhrase improves audio-to-image alignment and consistently enhances generation quality by mitigating semantic misalignment.¹

CCS Concepts

• Information systems → Multimedia content creation.

Keywords

Audio to Image Generation, Diffusion Model, Multi-modal Representation, Language-guided Generation

1 Introduction

With the recent advances in text-to-image generation [30, 39, 41, 43], there has been growing interest in extending pre-trained models by adding new modalities without end-to-end retraining [3, 24, 35, 53]. Among these, audio-to-image generation [3, 22, 46, 51] has gained attention for its potential for cross-modal generation, enabled by advances in multi-modal encoders [12, 13, 50]. To enable audio-based conditioning, recent work [35, 51] proposed transferring knowledge from a text encoder to an audio encoder using an audio-text paired dataset. However, due to the scarcity and difficulty of collecting detailed captions for audio, GlueGen [35] instead utilized audio classification datasets (i.e., audio-category pairs) by combining each class label with simple CLIP [36]-style prompt templates.

*Corresponding author.

¹Project page: <https://github.com/komjii2/CatchPhrase>

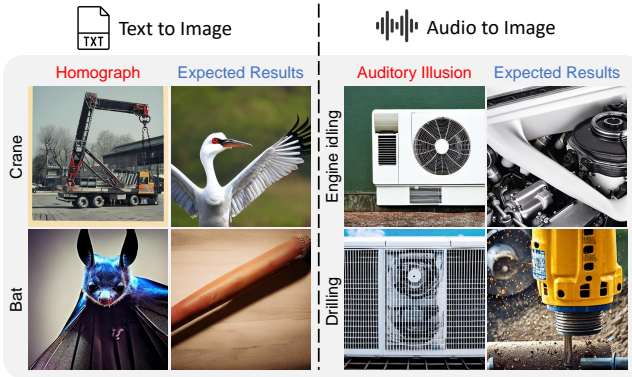


Figure 2: Examples of cross-modal misalignment. When the prompts “crane” and “bat” are used for image generation, the model often confuses their meanings, resulting in class-level misalignment (i.e., homographs). Similarly, given audio samples such as “engine idling” or “drilling,” the model produces instance-level misaligned results due to auditory illusions.

Although GlueGen [35] showed notable performance in audio-to-image generation, we observe that relying on a simple fixed template introduces two types of semantic misalignment: a class-level linguistic misalignment and an instance-level auditory misalignment, as illustrated in Fig. 2. First, the linguistic misalignment arises from phenomena such as *homographs* (or polysemy), a problem previously identified in text-to-image generation [10]. As shown in the left part of Fig. 2, the model sometimes confuses words like “crane” and “bat,” leading to mismatched image outputs. This occurs because audio classification datasets consist of simple labels that lack sufficient semantic information to disambiguate between identical words with different meanings. Second, at the instance level, auditory misalignment like *auditory illusion* arises due to limited semantic cues in audio signals, making classification less reliable. For instance, even when input sounds are clearly distinguishable to humans, the model often fails to capture such perceptual differences, as shown in the right part of Fig. 2. While auditory misalignment is widely observed in diverse perceptual phenomena, our focus is on these general-context misalignments, rather than phoneme-level effects such as the McGurk effect [25], which involve mismatches between auditory and visual speech cues.

Based on these observations, we hypothesize that enriching each class with appropriate semantic information can help reduce the inherent misalignment arising from the limited expressiveness of class labels in audio classification datasets. To improve semantic alignment in audio-to-image generation, we propose **CatchPhrase**, which utilizes audio-informed and context-rich prompts to mitigate cross-modal misalignment. However, crafting such prompts with diverse contextual details for every class is labor-intensive. To automate the generation of meaningful, audio-informed prompts from weak labels, we extract Enriched Cross-modal Prompts (EXPrompt), leveraging class-related knowledge from large language models (LLMs) [32, 37, 38] and audio captioning models (ACMs) [17]. Specifically, we construct semantically enriched text prompts by querying LLMs with inputs composed of three perspectives (visual, auditory,

and semantic) combined with weak class labels. To further incorporate contextual cues from the audio itself, we add enriched audio prompts using zero-shot ACMs. EXPrompts capture a wide range of class-relevant contextual information.

To enhance semantic alignment and assign appropriate prompts to each audio input, we introduce EXPrompt Selector, a multi-modal aware filtering and retrieval strategy. We first compute the relevance scores between EXPrompts and an audio subset within the same class from the audio classification dataset, filtering out class-irrelevant prompts. This process mitigates class-level misalignment, such as confusion caused by homographs, and ensures that each audio class is aligned with contextually appropriate prompts. To further address instance-level misalignment arising from perceptual discrepancies, such as auditory illusions, we apply a retrieval step. For each audio sample, we compute its similarity with the filtered prompt set within the same class and retrieve the prompt that is most semantically aligned. This enables fine-grained alignment by reflecting subtle variations across audio samples within the same class and pairs each audio input with a prompt that best reflects its semantic context. By grounding each audio input in a more accurate textual description, the generation model becomes more robust to perceptual inconsistencies.

Finally, we train our model using the InfoNCE loss, encouraging the generation model to produce semantically aligned images when given audio inputs while mitigating cross-modal misalignment. We validate the effectiveness of our method on various audio classification datasets, including UrbanSound8K (US8K) [44], ESC50 [33], and VGGSound [8]. Our model successfully captures semantic cues from both text and audio, effectively mitigating cross-modal misalignment, such as homographs and auditory illusions, in extensive experiments. In conclusion, our contributions are as follows:

- We propose **CatchPhrase**, an audio-to-image generation framework that explicitly addresses cross-modal misalignment. To the best of our knowledge, this is the first work to tackle auditory illusions directly in this context.
- We introduce EXPrompts, enriched prompts that compensate for the lack of semantic detail in conventional audio classification labels.
- We design a multi-modal-aware selector that pairs each audio sample with a semantically precise and contextually aligned prompt, improving semantic alignment during training.
- Extensive experiments on multiple audio classification datasets validate the effectiveness of our method in reducing cross-modal misalignment.

2 Related Work

2.1 LLMs Descriptions For Downstream Task

Recently, with the remarkable performance of Large Language Models (LLMs) such as GPT [2, 6] in the field of language understanding, many researchers have leveraged LLMs for various vision and language tasks [1, 9, 16, 23, 27, 34, 42]. CuPL [34] extracts appearance descriptions of each class through GPT-3 and utilizes them for better zero-shot image classification. Further, [1] enhances zero-shot classification performance by leveraging enriched descriptions not only from text but also from visual inputs. In image generation

fields, [14] optimizes text prompts using LLMs, guiding Stable Diffusion [41] to generate better-quality images. Instructpix2pix [5] and WavCaps [26] create a dataset using descriptions from GPT [6], enabling image editing through human instructions. Audio Journey[28] leverages enriched captions from Alpaca [47] to augment weakly labeled audio datasets in text-to-audio generation tasks. Our work builds on this approach but differs by leveraging multi-modal cues to generate semantically enriched prompts.

2.2 Audio-to Image Generation

Advancements in multi-modal learning have enabled the alignment of diverse modalities such as text, audio, and image within a shared embedding space. CLIP [36] jointly embeds text and image, supporting a wide range of downstream tasks, including conditional image generation [41, 43] and cross-modal retrieval [54]. Several approaches extend this representation space to include audio [11–13, 49], training audio encoders to align with the vision-language space. These unified representations also facilitate conditional image generation from audio, which has led to significant advances in audio-to-image generation [3, 21, 35, 45, 51]. Some methods use CLAP [11] for audio-conditioned image generation [3, 45], while others rely on AudioCLIP [13] to achieve similar goals [21, 35, 51]. In this work, we build upon these multi-modal encoders for audio-to-image generation and focus on improving their capability to resolve cross-modal ambiguities.

2.3 Enhancing Semantic Alignment

In various generative tasks, including captioning and image synthesis, many studies have focused on improving semantic alignment between visual content and language. For example, prior work [18, 19, 31, 40, 52] addresses the limitations of diffusion models in accurately reflecting textual prompts, enhancing text-image correspondence through attention alignment, interpretability, or inference-time guidance. Additionally, studies such as [7, 29] highlight that verb semantics—especially those involving human-object interactions—are often underrepresented in generated images. To address this, they propose training strategies that explicitly account for verb-specific structures. In the video domain, AADiff [20] tackles temporal ambiguity by incorporating auxiliary audio signals to disambiguate motion, demonstrating the effectiveness of multimodal cues in resolving under-specified linguistic inputs.

Inspired by these insights, our approach leverages both audio and text as complementary modalities to disambiguate audio-to-image generation and improve cross-modal semantic consistency.

3 CatchPhrase

Our goal is to help audio-to-image generation models mitigate cross-modal misalignment, such as homographs and auditory illusions. Our proposed method, **CatchPhrase**, illustrated in Fig. 3, consists of three main components. First, we generate Enriched Cross-modal Prompts (EXPrompts) by leveraging class-relevant knowledge from large language models (LLMs) and audio captioning models (ACMs). These prompts enrich the weak labels in audio classification datasets by capturing diverse and detailed semantic information. Second, we introduce the EXPrompt Selector, a multi-modal-aware filtering and retrieval strategy designed to reduce

cross-modal misalignment. It aligns each audio sample with the most semantically relevant prompt by addressing both class-level and instance-level misalignment. Finally, we train a lightweight mapping network using the enriched audio-text pairs, where the selected prompts act as semantic anchors to guide cross-modal alignment.

3.1 Preliminary

To condition audio inputs into pre-trained text-to-image generation model, GlueGen [35] introduces a mapping network $M(\cdot)$ that aligns features from an audio encoder $AE(\cdot)$ [13] with those from a text encoder $TE(\cdot)$ [36]. The mapping network is trained using paired text X^p and audio X^a samples from an audio classification dataset with three objectives. First, features are extracted using the encoders as $f^t = TE(X^p)$ and $f^a = AE(X^a)$. To minimize the element-wise discrepancy between f^t and the mapped audio feature $M(f^a)$, they utilize a mean squared error (MSE) loss:

$$\mathcal{L}_{mse} = \mathbb{E}_{(X^p, X^a)} [\|f^t - M(f^a)\|_2^2] \quad (1)$$

In order to preserve the original information from f^a , they introduce a reconstruction loss using a decoder network $N(\cdot)$:

$$\mathcal{L}_{rec} = \mathbb{E}_{X^a} [\|f^a - N(M(f^a))\|_2^2] \quad (2)$$

Finally, they apply an adversarial loss with a discriminator network $D(\cdot)$ to align the overall distribution between f^t and $M(f^a)$:

$$\mathcal{L}_{adv} = \mathbb{E}_{X^p} [\log D(f^t)] + \mathbb{E}_{X^a} [\log(1 - D(M(f^a)))] \quad (3)$$

3.2 EXPrompt Mining

To enrich weak labels with semantic details in audio classification datasets, we generate semantically enriched cross-modal prompts by leveraging both textual and auditory cues, as shown in Fig. 4. Specifically, we extract text-informed and audio-derived rich prompts using large language models (LLMs) and audio captioning models (ACMs), respectively. First, we obtain class-relevant rich prompts using GPT-3.5 [32]. Inspired by the findings of [34], we design three types of queries—visual, auditory, and semantic—to capture class-relevant contextual information from LLMs. The visual and auditory queries guide the LLM to describe observable features such as object appearance or characteristic sound patterns commonly associated with the class. In contrast, the semantic query (e.g., “Create one sentence about meaning of a(n) class in real world.”) aims to reduce linguistic ambiguity (e.g., the word “siren”) by encouraging the generation of more specific, disambiguated, and semantically precise responses. The exact queries and the examples of EXPrompts are provided in the supplementary materials.

To additionally capture auditory cues, we generate audio-derived prompts using EnCLAP [17], a zero-shot audio captioning model. By combining prompts from both modalities, we construct a diverse and semantically rich candidate prompt set that facilitates more accurate cross-modal alignment.

3.3 EXPrompt Selector

To further mitigate cross-modal misalignment that may remain in the EXPrompts, we apply CLAP-based filtering and retrieval and pair the most semantically relevant prompts for each audio sample. This enables the audio-to-image generation model to understand

Algorithm 1 : EXPrompt Selector for Filtering

Require: Audio Subset embeddings and class label $\mathcal{A} = \{\mathbf{r}_i^a, \mathbf{c}_i\}_{i=1}^{N_{AS}}$,

Text embeddings and class label $\mathcal{T} = \{\mathbf{r}_j^p, \mathbf{c}_j\}_{j=1}^{N_{EXP}}$, Top-K parameter K

Ensure: Score matrix $S_F \in \mathbb{R}^{N_{AS} \times N_{EXP}}$, Top-K text embeddings per audio embedding

```
1: Initialize similarity matrix  $S_F \leftarrow \text{zeros}(N_{AS}, N_{EXP})$ 
2: for  $i = 1$  to  $N_{AS}$  do
3:    $\mathbf{r}_i^a, \mathbf{c}_i \leftarrow \mathcal{A}[i]$ 
4:   for  $j = 1$  to  $N_{EXP}$  do
5:      $\mathbf{r}_j^p, \mathbf{c}_j \leftarrow \mathcal{T}[j]$ 
6:     if  $\mathbf{c}_i == \mathbf{c}_j$  then
7:        $S[i][j] \leftarrow S[i][j] + \text{cosine similarity}(\mathbf{r}_i^a, \mathbf{r}_j^p)$ 
8:     else
9:        $S[i][j] \leftarrow S[i][j] + (1 - \text{cosine similarity}(\mathbf{r}_i^a, \mathbf{r}_j^p))$ 
10:    end if
11:  end for
12:   $I_{\text{top-K}}^{(i)} \leftarrow \text{top-K Indices}(S_F[i], K)$ 
13:   $\mathcal{T}_{\text{top-K}}^{(i)} \leftarrow \{\mathcal{T}[j] \mid j \in I_{\text{top-K}}^{(i)}\}$ 
14: end for
15: return  $S_F, \{\mathcal{T}_{\text{top-K}}^{(i)}\}_{i=1}^{N_{AS}}$ 
```

Algorithm 2 : EXPrompt Selector for Retrieval

Require: Audio embedding \mathbf{r}^a , Text embeddings $\mathcal{T} = \{\mathbf{r}_i^p\}_{i=1}^{N_F}$

Ensure: Score matrix $S_R \in \mathbb{R}^{N_F}$, Top-1 text embedding

```
1: Initialize similarity matrix  $S_R \leftarrow \text{zeros}(N_F)$ 
2: for  $i = 1$  to  $N_F$  do
3:    $\mathbf{r}_i^p \leftarrow \mathcal{T}[i]$ 
4:    $S_R[i] \leftarrow \text{cosine similarity}(\mathbf{r}^a, \mathbf{r}_i^p)$ 
5: end for
6:  $I_{\text{top-1}} \leftarrow \text{top-1 Indices}(S_R, 1)$ 
7:  $\mathcal{T}_{\text{top-1}} \leftarrow \{\mathcal{T}[i] \mid i \in I_{\text{top-1}}\}$ 
8: return  $S_R, \mathcal{T}_{\text{top-1}}$ 
```

supervise the training of the mapping network. Together, this two-stage refinement process ensures that prompts are semantically relevant and better aligned with audio inputs, thereby improving cross-modal consistency. The overall process of the EXPrompt Selector is summarized in Alg. 1 and Alg. 2.

3.4 Training Phase

We incorporate the InfoNCE [48] loss as an additional training objective to enhance cross-modal alignment, which is widely used for contrastive learning in representation learning frameworks. InfoNCE is designed to minimize the distance between a query and its corresponding positive sample while maximizing the distance to negative samples.

$$\mathcal{L}_{\text{InfoNCE}} = -\log \frac{\exp(\text{sim}(\mathbf{q}, \mathbf{k}^+)/\tau)}{\exp(\text{sim}(\mathbf{q}, \mathbf{k}^+)/\tau) + \sum_{\mathbf{k}^- \in \mathcal{N}} \exp(\text{sim}(\mathbf{q}, \mathbf{k}^-)/\tau)}, \quad (6)$$

where $\mathbf{q} \in \mathbb{R}^d$ denotes the query embedding vector obtained from a retrieved prompt. $\mathbf{k}^+ \in \mathbb{R}^d$ denotes the positive key from the same class as the query \mathbf{q} . $\mathcal{N} = \{\mathbf{k}_1^-, \mathbf{k}_2^-, \dots, \mathbf{k}_M^-\}$ is a set of negative keys that do not correspond to \mathbf{q} . $\text{sim}(\mathbf{q}, \mathbf{k})$ denotes a similarity function, typically cosine similarity, defined as $\frac{\mathbf{q}^\top \mathbf{k}}{\|\mathbf{q}\| \|\mathbf{k}\|}$. $\tau > 0$ is a temperature parameter that controls the sharpness of the distribution. Finally, we train only the mapping network with $\mathcal{L}_{\text{InfoNCE}}$ combined with Eq.1, Eq.2, and Eq. 3 losses as follows:

$$\mathcal{L}_{\text{total}} = \lambda_1 \mathcal{L}_{\text{mse}} + \lambda_2 \mathcal{L}_{\text{rec}} + \lambda_3 \mathcal{L}_{\text{adv}} + \lambda_4 \mathcal{L}_{\text{InfoNCE}}. \quad (7)$$

To balance the influence of different learning signals, we assign a separate weight $\lambda_1, \lambda_2, \lambda_3$ and λ_4 to each loss term, which is determined empirically.

4 Experiments

4.1 Experimental Setup

Training Configurations. Our method is trained on the Urban-Sound8K (US8K) [44], ESC-50 [33], and VGGSound [8] datasets using a single NVIDIA RTX A6000 GPU. For VGGSound, following the experimental setup in Sound2Scene [22], we use a subset of 50 selected classes. Images for evaluation are generated using Stable Diffusion v2.1 [41] with the PLMS sampler, and the random seed is fixed at 42 for reproducibility. During training, we use a learning rate and batch size of 5×10^{-5} and 8 for US8K, 1×10^{-4} and 32 for ESC50, and 5×10^{-4} and 256 for VGGSound. The loss weights $\lambda_1, \lambda_2, \lambda_3$, and λ_4 are set to 1.0, 10000, 10000, and 0.5, respectively. For the InfoNCE loss, we use 8 negative samples \mathcal{N} and set the temperature parameter τ to 0.8.

Evaluation Metrics. Since CLIP [36] includes only text and image encoders, it is not inherently suitable for measuring the similarity between input audio and generated images. Following [51], we adopt the Audio-Image Similarity (AIS) metric to evaluate cross-modal alignment between audio inputs and image outputs. In addition, we use Frechet Inception Distance (FID) [15] and Kernel Inception Distance (KID) [4] to assess the visual quality of the generated images. Additional evaluation metrics, such as retrieval performance or user studies, are provided in the supplementary material.

4.2 Comparisons with Previous Methods

We compare CatchPhrase with Sound2Scene [46], SonicDiffusion [3], and GlueGen [35] in Tab. 1, all comparative experiments were conducted on the US8K, ESC50, and VGGSound50 datasets. We report AIS scores only for US8K and ESC50, as these datasets contain audio-text pairs without corresponding images. As shown in the table, our model consistently outperforms the baselines across all datasets. This result suggests that EXPrompts effectively help the generation model address both class-level and instance-level misalignment.

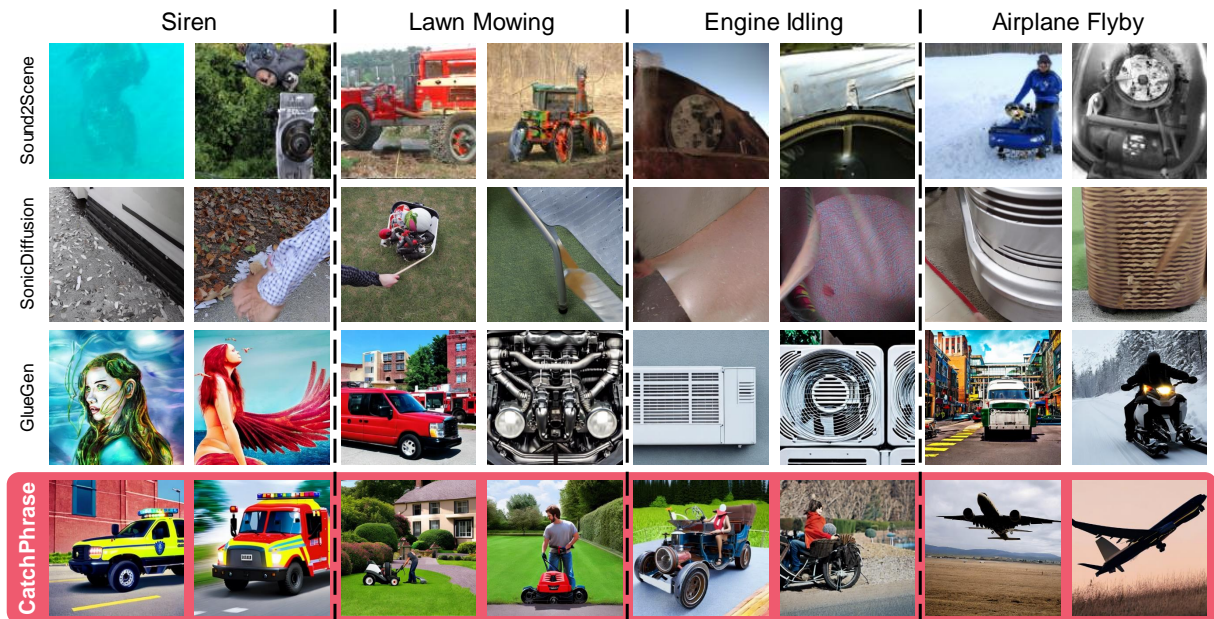


Figure 5: Comparison of image results between previous works and CatchPhrase, demonstrating enhanced semantic alignment. Images with a pink borderline are generated using CatchPhrase. CatchPhrase generates semantically accurate images, unlike prior methods that struggle with homographs (e.g., “siren”) and auditory illusions (e.g., “lawn mowing,” “engine idling,” and “airplane flyby”).

Table 1: Quantitative comparison between existing audio to image generation methods and CatchPhrase on various audio classification dataset. Bolded numbers indicate the best performance, and underlined numbers represent the second-best scores across the compared methods.

| | US8K | ESC50 | VGGSound | | |
|--------------------|--------------|--------------|--------------|--------------|--------------|
| | AIS (↑) | AIS (↑) | AIS (↑) | FID (↓) | KID (↓) |
| Sound2Scene [22] | .0842 | .1009 | .1080 | 87.04 | .0236 |
| GlueGen [35] | <u>.1444</u> | <u>.1918</u> | <u>.1950</u> | 76.66 | .0188 |
| SonicDiffusion [3] | .0814 | .0624 | .0621 | <u>68.98</u> | <u>.0136</u> |
| CatchPhrase | .1910 | .2423 | .2017 | 65.62 | .0119 |

We also visualize qualitative results in Fig. 5. Unlike previous methods that often misalign the audio semantics, our model successfully generates images that match the corresponding audio inputs. In particular, CatchPhrase accurately generates the image for “siren,” compared to GlueGen, demonstrating its ability to resolve class-level ambiguity such as homographs.

4.3 Ablation Studies

Component Ablation Studies. To evaluate the effectiveness of each component in CatchPhrase, we conduct a series of ablation studies comparing the template-based baseline with different configurations of our model. As shown in Tab. 2, incorporating both filtering and retrieval leads to a clear improvement in audio-image alignment, demonstrating their complementary roles. Moreover, the qualitative results in Fig. 6 further support this finding, illustrating that CatchPhrase produces more accurate and semantically

Table 2: Ablation studies for the CatchPhrase component. Assessing the impact of applying EXPrompt, filtering F and retrieval R . We evaluate various dataset on AIS score. Higher is better.

| Method | EXPrompt | F | R | US8K | ESC50 | VGGSound |
|--------------|----------|-----|-----|--------------|--------------|--------------|
| GlueGen [35] | | | | .1444 | .1918 | .1950 |
| CatchPhrase | ✓ | | | .0902 | .0876 | .0957 |
| CatchPhrase | ✓ | ✓ | | .1117 | .2005 | .1766 |
| CatchPhrase | ✓ | | ✓ | .1427 | .1570 | .1906 |
| CatchPhrase | ✓ | ✓ | ✓ | .1910 | .2423 | .2017 |

Table 3: Ablation studies for queries. Class-based EXPrompt mining is conducted with different types of queries: V (visual), A (auditory), and S (semantic).

| Method | V | A | S | AIS (↑) |
|--------------|-----|-----|-----|--------------|
| GlueGen [35] | | | | .1444 |
| (a) | ✓ | | | .1671 |
| (b) | | ✓ | | .1529 |
| (c) | | | ✓ | .1625 |
| (d) | ✓ | | ✓ | .1574 |
| (e) | | ✓ | ✓ | .1590 |
| Ours | ✓ | ✓ | ✓ | .1910 |

aligned images compared to its ablated variants. Overall, these results highlight the critical role of each component in achieving better performance.

Query Ablation Studies. We investigate how different types of concept queries affect the final audio-visual alignment in Tab. 3. As shown in the table, using all three query types—visual, auditory,

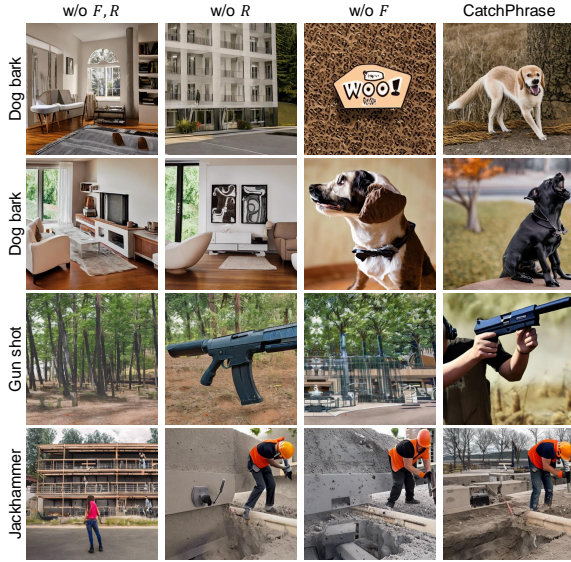


Figure 6: Qualitative results from the CatchPhrase component ablation study. Without applying filtering, prompts such as “woof woof” may be semantically close but serve as noisy and cumbersome inputs from the perspective of image generation. Removing the retrieval component from CatchPhrase results in a loss of semantic precision during training.

Table 4: Ablation studies for CatchPhrase design choices. We design four different variations of the CatchPhrase process, each of which is illustrated in the supplementary materials.

| Method | AIS (\uparrow) |
|--------------------------------------|-----------------------|
| CatchPhrase (Audio-only filtering) | .1636 (+.0192) |
| CatchPhrase (Text-only filtering) | .1724 (+.0280) |
| CatchPhrase (Merge after filtering) | .1707 (+.0263) |
| CatchPhrase (Merge before filtering) | .1910 (+.0466) |

and semantic—yields the best performance. A notable finding is that using only auditory queries leads to the lowest performance. This is because auditory prompts tend to produce rich prompts containing onomatopoeic expressions (e.g., “woof”), which often lack semantic detail useful for image generation. Consequently, such prompts result in suboptimal outputs. We provide examples generated using only auditory queries in the supplementary materials.

Filtering Equation Ablation Studies. As shown in Eq. 4, the filtering score consists of two main components: the first measures the similarity between a prompt and audio samples from the same class, while the second measures similarity to audio samples from different classes. To evaluate the effectiveness of the second term, we conduct experiments on the US8K dataset using class-based EXPrompts. As presented in Tab. 5, incorporating the similarity term for different classes improves audio-image alignment. We attribute this to the fact that rich prompts occasionally contain details relevant to multiple classes, which may dilute class-specific semantics. By penalizing prompts that are overly similar to audio

Table 5: Effect of penalizing cross-class similarity in relevance scoring. Penalizing prompts that are overly similar to audio samples from other classes helps filter out semantically ambiguous candidates, improving class-level disambiguation.

| Method | AIS (\uparrow) |
|---------------------------------|-----------------------|
| CatchPhrase (w/o negative term) | .1652 (+.0208) |
| CatchPhrase | .1910 (+.0466) |

Table 6: The effect of leveraging InfoNCE objective. We evaluate various dataset on AIS score. Higher is better.

| Method | US8K | ESC50 | VGGSound |
|---------------------------|--------------|--------------|--------------|
| CatchPhrase (w/o InfoNCE) | .1905 | .2422 | .2010 |
| CatchPhrase (Ours) | .1910 | .2423 | .2017 |

from other classes, the filtering mechanism effectively reduces cross-class semantic contamination.

Component Sequence Ablation Studies. As shown in Fig. 3, CatchPhrase consists of three main stages: rich prompt generation, filtering, and retrieval. Each component can be flexibly configured depending on the modality and filtering strategy.

First, users may choose between using both audio and text inputs from the audio classification dataset or adopting a uni-modal approach. In the uni-modal setting, using only audio results in *audio-only filtering*, while using only text leads to *text-only filtering*. The filtering process involves two hyperparameters, N_{as} and N_{ft} , which are selected empirically; corresponding experiments are included in the appendices. After generating rich prompts, another design choice involves the point at which to apply filtering. In the *merge-before-filtering* strategy, audio- and text-based prompts are first combined and then filtered. Conversely, *merge-after-filtering* applies filtering to each modality independently before merging.

As shown in Tab. 4, the merge-before-filtering strategy achieves superior performance. This improvement is attributed to the ability of text-based prompts to suppress noise introduced by audio-based prompts, which are more susceptible to auditory illusions caused by audio captioning models (ACMs). Filtering each modality separately may lead to cross-modal ambiguity, as noisy prompts from the audio stream can contaminate the final prompt set. In contrast, filtering after merging promotes the selection of semantically richer and more reliable prompts.

Objective Function Ablation Studies. Leveraging the filtered EXPrompts obtained through EXPrompt Selector for filtering within the InfoNCE loss contributes to mitigating auditory illusions. In contrast to the homograph issue, which occurs at the class level, auditory illusions arise at the instance level, making them more sensitive to sample-specific ambiguity. This effect is empirically validated in Tab. 6 and Fig. 7.

Audio Captioning Models with Image Generation. Audio-to-image generation using audio captioning models (ACMs) can be approached in several ways. First, captions for all audio samples in an audio classification dataset can be pre-generated using ACMs and used for one-to-one supervised training. Second, the pre-generated captions can serve as direct inputs to a text-to-image generation model, enabling a two-stage audio-to-image generation pipeline.



Figure 7: Comparison of image results with and without the use of InfoNCE loss. This shows the effectiveness of prompt-guided contrastive learning in enhancing semantic alignment.

Table 7: Ablation on audio caption to image generation. We evaluate various frameworks that can use text descriptions extracted from audio inputs.

| Method | AIS (↑) |
|--------------------------------------|--------------|
| GlueGen [35] | .1444 |
| GlueGen (w/ Audio Caption) | .1307 |
| EnCLAP [17]+Stable Diffusion2.1 [41] | .1695 |
| CatchPhrase | .1910 |

We compare these two approaches with CatchPhrase on the US8K dataset. As reported in Tab. 7, CatchPhrase outperforms both ACM-based methods in terms of AIS scores. These results suggest that the inferior performance of ACM-based approaches stems from inaccurate or ambiguous captions, likely caused by auditory illusions during audio-only filtering. They also demonstrate that directly using such captions as prompts in a text-to-image generation model is less effective than training an audio-to-image model that learns the underlying semantics of the audio input.

Effectiveness of EXPrompts. We investigate the impact of rich prompts on image generation compared to template-based prompts in Fig. 8. The ESC50 dataset contains simpler class labels than US8K or VGGSound, with sounds such as “gunshot” or “dog bark” labeled simply as “gun” or “dog.”

As can be seen, template-based prompts often fail to capture the full context of the audio input, leading to less accurate visual representations. In contrast, CatchPhrase generates rich, context-aware descriptions based on both audio and text inputs, enabling more faithful image generation. For example, even when the audio



Figure 8: Impact of EXPrompts on image generation compared to template-based prompts. Images with a white borderline are generated using template-based prompts, while images with a pink borderline are generated using CatchPhrase.

input corresponds to the word “gun,” CatchPhrase generates an image of a gun emitting sparks, effectively reflecting the sound of a gunshot. Similarly, for the class “dog,” it generates an image of a barking dog that aligns with the audio input. This demonstrates that EXPrompts enrich the semantic information of weak labels in conventional audio classification datasets, thereby improving semantic alignment between audio and text.

5 Conclusion

We propose CatchPhrase, a framework designed to address cross-modal misalignment in audio-to-image generation, particularly those stemming from weak labels and ambiguous audio in audio classification datasets. By leveraging large language models (LLMs) and audio captioning models (ACMs), our method generates a diverse set of enriched prompts without relying on predefined templates, thereby reducing manual effort. To further alleviate residual misalignment, we introduce a multimodal-aware filtering mechanism that selects semantically appropriate prompts for training the encoder adaptor. Extensive experiments on multiple datasets validate the effectiveness of our approach, demonstrating consistent improvements in both quantitative metrics and qualitative results.

Acknowledgments

This was partly supported by the Institute of Information & Communications Technology Planning & Evaluation (IITP) grant funded by the Korean government(MSIT) (No.RS-2020-II201373, Artificial Intelligence Graduate School Program(Hanyang University)) and the Institute of Information & Communications Technology Planning & Evaluation (IITP) grant funded by the Korean government(MSIT)

(No.RS-2025-02219062, Self-training framework for VLM-based defect detection and explanation model in manufacturing process).

References

- [1] Abdelrahman Abdelhamed, Mahmoud Afifi, and Alec Go. 2024. What Do You See? Enhancing Zero-Shot Image Classification with Multimodal Large Language Models. *arXiv preprint arXiv:2405.15668* (2024).
- [2] Josh Achiam, Steven Adler, Sandhini Agarwal, Lama Ahmad, Ilge Akkaya, Florencia Leoni Aleman, Diogo Almeida, Janko Altmenschmidt, Sam Altman, Shyamal Anadkat, et al. 2023. GPT-4 Technical Report. *arXiv preprint arXiv:2303.08774* (2023).
- [3] Burak Can Biner, Farrin Marouf Sofian, Umur Berkay Karakaş, Duygu Ceylan, Erkut Erdem, and Aykut Erdem. 2024. SonicDiffusion: Audio-Driven Image Generation and Editing with Pretrained Diffusion Models. *arXiv preprint arXiv:2405.00878* (2024).
- [4] Mikołaj Bińkowski, Danica J. Sutherland, Michael Arbel, and Arthur Gretton. 2021. Demystifying MMD GANs. *arXiv:1801.01401 [stat.ML]* <https://arxiv.org/abs/1801.01401>
- [5] Tim Brooks, Aleksander Holynski, and Alexei A Efros. 2023. Instructpix2pix: Learning to follow image editing instructions. In *Proceedings of the IEEE/CVF Conference on Computer Vision and Pattern Recognition*. 18392–18402.
- [6] Tom Brown, Benjamin Mann, Nick Ryder, Melanie Subbiah, Jared D Kaplan, Prafulla Dhariwal, Arvind Neelakantan, Pranav Shyam, Girish Sastry, Amanda Askell, et al. 2020. Language models are few-shot learners. *Advances in neural information processing systems* 33 (2020), 1877–1901.
- [7] Seungju Cha, Kwanyoung Lee, Ye-Chan Kim, Hyunwoo Oh, and Dong-Jin Kim. 2025. VerbDiff: Text-Only Diffusion Models with Enhanced Interaction Awareness. *arXiv:2503.16406 [cs.GR]* <https://arxiv.org/abs/2503.16406>
- [8] Honglie Chen, Weidi Xie, Andrea Vedaldi, and Andrew Zisserman. 2020. Vgsgound: A large-scale audio-visual dataset. In *ICASSP 2020-2020 IEEE International Conference on Acoustics, Speech and Signal Processing (ICASSP)*. IEEE, 721–725.
- [9] Mia Chiquier, Utkarsh Mall, and Carl Vondrick. 2025. Evolving interpretable visual classifiers with large language models. In *European Conference on Computer Vision*. Springer, 183–201.
- [10] Chengbin Du, Yanxi Li, Zhongwei Qiu, and Chang Xu. 2024. Stable diffusion is unstable. *Advances in Neural Information Processing Systems* 36 (2024).
- [11] Benjamin Elizalde, Soham Deshmukh, Mahmoud Al Ismail, and Huaming Wang. 2023. Clap learning audio concepts from natural language supervision. In *ICASSP 2023-2023 IEEE International Conference on Acoustics, Speech and Signal Processing (ICASSP)*. IEEE, 1–5.
- [12] Rohit Girdhar, Alaaeldin El-Nouby, Zhuang Liu, Mannat Singh, Kalyan Vasudev Alwala, Armand Joulin, and Ishan Misra. 2023. Imagebind: One embedding space to bind them all. In *Proceedings of the IEEE/CVF Conference on Computer Vision and Pattern Recognition*. 15180–15190.
- [13] Andrey Guzhov, Federico Raue, Jörn Hees, and Andreas Dengel. 2022. Audioclip: Extending clip to image, text and audio. In *ICASSP 2022-2022 IEEE International Conference on Acoustics, Speech and Signal Processing (ICASSP)*. IEEE, 976–980.
- [14] Yaru Hao, Zewen Chi, Li Dong, and Furu Wei. 2024. Optimizing prompts for text-to-image generation. *Advances in Neural Information Processing Systems* 36 (2024).
- [15] Martin Heusel, Hubert Ramsauer, Thomas Unterthiner, Bernhard Nessler, and Sepp Hochreiter. 2018. GANs Trained by a Two Time-Scale Update Rule Converge to a Local Nash Equilibrium. *arXiv:1706.08500 [cs.LG]* <https://arxiv.org/abs/1706.08500>
- [16] Yushi Hu, Hang Hua, Zhengyuan Yang, Weijia Shi, Noah A Smith, and Jiebo Luo. 2022. Promptcap: Prompt-guided task-aware image captioning. *arXiv preprint arXiv:2211.09699* (2022).
- [17] Jaeyeon Kim, Jaeyoon Jung, Jinjoo Lee, and Sang Hoon Woo. 2024. Enclap: Combining neural audio codec and audio-text joint embedding for automated audio captioning. In *ICASSP 2024-2024 IEEE International Conference on Acoustics, Speech and Signal Processing (ICASSP)*. IEEE, 6735–6739.
- [18] Si-Woo Kim, Minju Jeon, Ye-Chan Kim, Soeun Lee, Taewhan Kim, and Dong-Jin Kim. 2025. SynC: Synthetic Image Caption Dataset Refinement with One-to-many Mapping for Zero-shot Image Captioning. In *Proceedings of the 33rd ACM International Conference on Multimedia*.
- [19] Ye-Chan Kim, Seungju Cha, Si-Woo Kim, Taewhan Kim, and Dong-Jin Kim. 2025. SIDA: Synthetic Image Driven Zero-shot Domain Adaptation. In *Proceedings of the 33rd ACM International Conference on Multimedia*.
- [20] Seungwoo Lee, Chaerin Kong, Donghyeon Jeon, and Nojun Kwak. 2023. AADiff: Audio-Aligned Video Synthesis with Text-to-Image Diffusion. *arXiv:2305.04001 [cs.CV]* <https://arxiv.org/abs/2305.04001>
- [21] Seung Hyun Lee, Wonseok Roh, Wonmin Byeon, Sang Ho Yoon, Chanyoung Kim, Jinkyu Kim, and Sangpil Kim. 2022. Sound-guided semantic image manipulation. In *Proceedings of the IEEE/CVF conference on computer vision and pattern recognition*. 3377–3386.
- [22] Taeyeon Lee, Jeonghun Kang, Hyeonyu Kim, and Taehwan Kim. 2023. Generating Realistic Images from In-the-wild Sounds. *arXiv:2309.02405 [cs.CV]* <https://arxiv.org/abs/2309.02405>
- [23] Rongjie Li, Yu Wu, and Xuming He. 2024. Learning by Correction: Efficient Tuning Task for Zero-Shot Generative Vision-Language Reasoning. In *Proceedings of the IEEE/CVF Conference on Computer Vision and Pattern Recognition*. 13428–13437.
- [24] Yuheng Li, Haotian Liu, Qingyang Wu, Fangzhou Mu, Jianwei Yang, Jianfeng Gao, Chunyuan Li, and Yong Jae Lee. 2023. Gligen: Open-set grounded text-to-image generation. In *Proceedings of the IEEE/CVF Conference on Computer Vision and Pattern Recognition*. 22511–22521.
- [25] Harry McGurk and John MacDonald. 1976. Hearing lips and seeing voices. *Nature* 264, 5588 (1976), 746–748.
- [26] Xinhao Mei, Chutong Meng, Haohe Liu, Qiuqiang Kong, Tom Ko, Chengqi Zhao, Mark D Plumbley, Yuexian Zou, and Wenwu Wang. 2024. Wavcaps: A chatgpt-assisted weakly-labelled audio captioning dataset for audio-language multimodal research. *IEEE/ACM Transactions on Audio, Speech, and Language Processing* (2024).
- [27] Sachit Menon and Carl Vondrick. 2022. Visual Classification via Description from Large Language Models. *arXiv:2210.07183 [cs.CV]* <https://arxiv.org/abs/2210.07183>
- [28] Jackson Michaels, Juncheng B Li, Laura Yao, Lijun Yu, Zach Wood-Doughty, and Florian Metze. 2024. Audio-Journey: Open Domain Latent Diffusion Based Text-To-Audio Generation. In *ICASSP 2024-2024 IEEE International Conference on Acoustics, Speech and Signal Processing (ICASSP)*. IEEE, 6960–6964.
- [29] Liliane Momeni, Mathilde Caron, Arsha Nagrani, Andrew Zisserman, and Cordelia Schmid. 2023. Verbs in Action: Improving verb understanding in video-language models. *arXiv:2304.06708 [cs.CV]* <https://arxiv.org/abs/2304.06708>
- [30] Alex Nichol, Prafulla Dhariwal, Aditya Ramesh, Pranav Shyam, Pamela Mishkin, Bob McGrew, Ilya Sutskever, and Mark Chen. 2021. Glide: Towards photorealistic image generation and editing with text-guided diffusion models. *arXiv preprint arXiv:2112.10741* (2021).
- [31] Yuta Oshima, Masahiro Suzuki, Yutaka Matsuo, and Hiroki Furuta. 2025. Inference-Time Text-to-Video Alignment with Diffusion Latent Beam Search. *arXiv:2501.19252 [cs.CV]* <https://arxiv.org/abs/2501.19252>
- [32] Long Ouyang, Jeff Wu, Xu Jiang, Diogo Almeida, Carroll L. Wainwright, Pamela Mishkin, Chong Zhang, Sandhini Agarwal, Katarina Slama, Alex Ray, John Schulman, Jacob Hilton, Fraser Kelton, Luke Miller, Maddie Simens, Amanda Askell, Peter Welinder, Paul Christiano, Jan Leike, and Ryan Lowe. 2022. Training language models to follow instructions with human feedback. *arXiv:2203.02155 [cs.CL]* <https://arxiv.org/abs/2203.02155>
- [33] Karol J Piczak. 2015. ESC: Dataset for environmental sound classification. In *Proceedings of the 23rd ACM international conference on Multimedia*. 1015–1018.
- [34] Sarah Pratt, Ian Covert, Rosanne Liu, and Ali Farhadi. 2023. What does a platypus look like? generating customized prompts for zero-shot image classification. In *Proceedings of the IEEE/CVF International Conference on Computer Vision*. 15691–15701.
- [35] Can Qin, Ning Yu, Chen Xing, Shu Zhang, Zeyuan Chen, Stefano Ermon, Yun Fu, Caiming Xiong, and Ran Xu. 2023. Gluegen: Plug and play multi-modal encoders for x-to-image generation. In *Proceedings of the IEEE/CVF International Conference on Computer Vision*. 23085–23096.
- [36] Alec Radford, Jong Wook Kim, Chris Hallacy, Aditya Ramesh, Gabriel Goh, Sandhini Agarwal, Girish Sastry, Amanda Askell, Pamela Mishkin, Jack Clark, et al. 2021. Learning transferable visual models from natural language supervision. In *International conference on machine learning*. PMLR, 8748–8763.
- [37] Alec Radford, Karthik Narasimhan, Tim Salimans, Ilya Sutskever, et al. 2018. Improving language understanding by generative pre-training. (2018).
- [38] Alec Radford, Jeffrey Wu, Rewon Child, David Luan, Dario Amodei, Ilya Sutskever, et al. 2019. Language models are unsupervised multitask learners. *OpenAI blog* 1, 8 (2019), 9.
- [39] Aditya Ramesh, Prafulla Dhariwal, Alex Nichol, Casey Chu, and Mark Chen. 2022. Hierarchical text-conditional image generation with clip latents. *arXiv preprint arXiv:2204.06125* 1, 2 (2022), 3.
- [40] Royi Rassin, Eran Hirsch, Daniel Glickman, Shauli Ravfogel, Yoav Goldberg, and Gal Chechik. 2023. Linguistic binding in diffusion models: Enhancing attribute correspondence through attention map alignment. *Advances in Neural Information Processing Systems* 36 (2023), 3536–3559.
- [41] Robin Rombach, Andreas Blattmann, Dominik Lorenz, Patrick Esser, and Björn Ommer. 2022. High-resolution image synthesis with latent diffusion models. In *Proceedings of the IEEE/CVF conference on computer vision and pattern recognition*. 10684–10695.
- [42] Noam Rotstein, David Bensaid, Shaked Brody, Roy Ganz, and Ron Kimmel. 2023. FuseCap: Leveraging Large Language Models for Enriched Fused Image Captions. *arXiv preprint arXiv:2305.17718* (2023).
- [43] Chitwan Saharia, William Chan, Saurabh Saxena, Lala Li, Jay Whang, Emily L Denton, Kamyar Ghasemipour, Raphael Gontijo Lopes, Burcu Karagol Ayan, Tim Salimans, et al. 2022. Photorealistic text-to-image diffusion models with deep language understanding. *Advances in neural information processing systems* 35 (2022), 36479–36494.

- [44] Justin Salamon, Christopher Jacoby, and Juan Pablo Bello. 2014. A dataset and taxonomy for urban sound research. In *Proceedings of the 22nd ACM international conference on Multimedia*. 1041–1044.
- [45] Kim Sung-Bin, Kim Jun-Seong, Junseok Ko, Yewon Kim, and Tae-Hyun Oh. 2024. SoundBrush: Sound as a Brush for Visual Scene Editing. arXiv:2501.00645 [cs.CV] <https://arxiv.org/abs/2501.00645>
- [46] Kim Sung-Bin, Arda Senocak, Hyunwoo Ha, Andrew Owens, and Tae-Hyun Oh. 2023. Sound to visual scene generation by audio-to-visual latent alignment. In *Proceedings of the IEEE/CVF Conference on Computer Vision and Pattern Recognition*. 6430–6440.
- [47] Rohan Taori, Ishaan Gulrajani, Tianyi Zhang, Yann Dubois, Xuechen Li, Carlos Guestrin, Percy Liang, and Tatsunori B. Hashimoto. 2023. Stanford Alpaca: An Instruction-following LLaMA model. https://github.com/tatsu-lab/stanford_alpaca.
- [48] Aaron van den Oord, Yazhe Li, and Oriol Vinyals. 2018. Representation learning with contrastive predictive coding. *arXiv preprint arXiv:1807.03748* (2018).
- [49] Ho-Hsiang Wu, Prem Seetharaman, Kundan Kumar, and Juan Pablo Bello. 2022. Wav2clip: Learning robust audio representations from clip. In *ICASSP 2022-2022 IEEE International Conference on Acoustics, Speech and Signal Processing (ICASSP)*. IEEE, 4563–4567.
- [50] Yusong Wu, Ke Chen, Tianyu Zhang, Yuchen Hui, Taylor Berg-Kirkpatrick, and Shlomo Dubnov. 2023. Large-scale contrastive language-audio pretraining with feature fusion and keyword-to-caption augmentation. In *ICASSP 2023-2023 IEEE International Conference on Acoustics, Speech and Signal Processing (ICASSP)*. IEEE, 1–5.
- [51] Guy Yariv, Itai Gat, Lior Wolf, Yossi Adi, and Idan Schwartz. 2023. AudioToken: Adaptation of Text-Conditioned Diffusion Models for Audio-to-Image Generation. arXiv:2305.13050 [cs.SD] <https://arxiv.org/abs/2305.13050>
- [52] Rushikesh Zawar, Shaurya Dewan, Prakanshul Saxena, Yingshan Chang, Andrew Luo, and Yonatan Bisk. 2024. DiffusionPID: Interpreting Diffusion via Partial Information Decomposition. arXiv:2406.05191 [cs.CV] <https://arxiv.org/abs/2406.05191>
- [53] Lvmin Zhang, Anyi Rao, and Maneesh Agrawala. 2023. Adding conditional control to text-to-image diffusion models. In *Proceedings of the IEEE/CVF International Conference on Computer Vision*. 3836–3847.
- [54] Mingyuan Zhang, Xinying Guo, Liang Pan, Zhongang Cai, Fangzhou Hong, Huirong Li, Lei Yang, and Ziwei Liu. 2023. Remodiffuse: Retrieval-augmented motion diffusion model. In *Proceedings of the IEEE/CVF International Conference on Computer Vision*. 364–373.

Supplementary Materials

Additional experimental details and analyses, which complement the main paper but were excluded due to space limitations, are provided in this supplementary material.

A Comparison of Image Generation Results Based on the Employed Queries

In experiment section, the use of audio queries is associated with a reduction in AIS performance. The observed quality degradation when utilizing only audio queries can be attributed to the model’s tendency to prioritize expressing the auditory characteristics of the given class label rather than incorporating visual information to guide image generation. As a result, the model often generates images that depict onomatopoeic expressions rather than faithfully constructing the intended objects, as illustrated in Fig. 9.

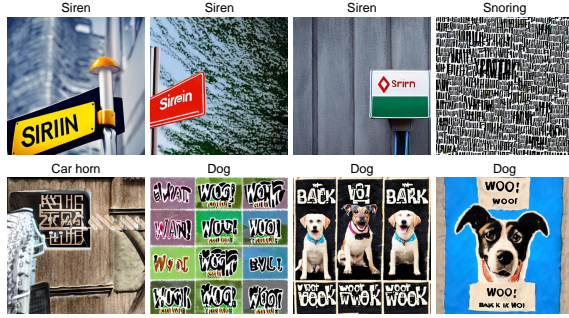


Figure 9: Generated images with using audio queries in text-based rich prompts. Onomatopoeic expressions and textual elements observed in images generated using EXPrompts crafted from audio queries, among text-based EXPrompts.

B EXPrompts with Paraphrasing

After filtering the EXPrompts, we use paraphrasing to augment the number of valuable prompts in *text-only filtering*. Paraphrasing leverages LLMs with the following query, similar to generating rich expression prompts. This process generates augmented prompts five times more than the number of filtered prompts used in retrieval along with the original filtered prompts. Filtering applies again, and related experiments reveal that paraphrasing does not significantly enhance performance. This outcome results from paraphrasing, altering only the style of sentences while maintaining the semantics of the already filtered prompts. This leads to minimal differences in outcomes, as shown in Tab 8. For comparison, CatchPhrase uses filtering hyper-parameters that sample 10 audio samples per class and select the top 10 prompts. The queries used for prompt augmentation are as follows:

Table 8: Quantitative comparison for applying paraphrase. P denotes paraphrasing, and F denotes filtering. The numbers in parentheses indicate the difference between AIS and GlueGen.

| Method | P | F | AIS |
|-----------------------------------|---|---|-----------------------|
| CatchPhrase (w/ P) | ✓ | | .1403 (-.0041) |
| CatchPhrase (w/ P, F) | ✓ | ✓ | .1584 (+.0140) |
| CatchPhrase (Text-only filtering) | | ✓ | .1724 (+.0280) |

- Summarize the following text in your own words: *prompt*
- Rewrite the following text that expresses the same idea in a different way: *prompt*
- Generate a paraphrase of the following text that expresses the same ideas in a different way: *prompt*
- Generate a paraphrase of the following text using different words and sentence structures while still conveying the same meaning: *prompt*
- Generate a summary or paraphrase of the following text that captures the essence of the ideas in a concise manner: *prompt*

C Component Sequence in CatchPhrase

The components of CatchPhrase can be configured in various combinations. To evaluate the effectiveness of each configuration, we measured the AIS for possible combinations. To facilitate a clearer understanding of these configurations, we have included Fig. 10 in the supplementary material. The *Merge before filtering* represents our most effective component configuration.

D Filtering Parameter

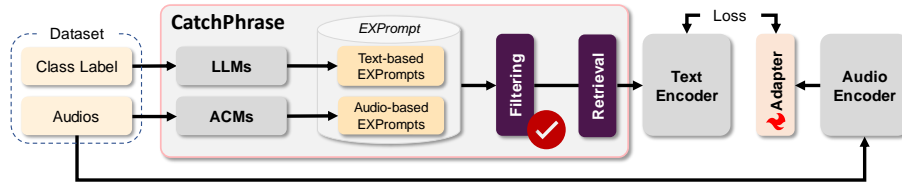
Among the filtering parameters, the choice of top-K yields intriguing experimental results as shown in Tab. 9. The top row shows the number of audio samples selected per class (N_{AS}) when constructing the audio subset. The first column shows the cutoff value for EXPrompts. The table values represent AIS scores. The middle row displays the AIS for text-based rich prompt filtering parameters, while the bottom row shows the AIS for audio-based rich prompt filtering parameters.

When different audio inputs from the same class are processed, a smaller value of N_{EXP} leads to a noticeable reduction in the diversity of the generated images. As illustrated in Fig. 11, a clear difference in diversity can be observed between the cases where $N_{EXP} = 1$ and $N_{EXP} = 20$ for audio inputs belonging to the “dog” and “engine idling” classes.

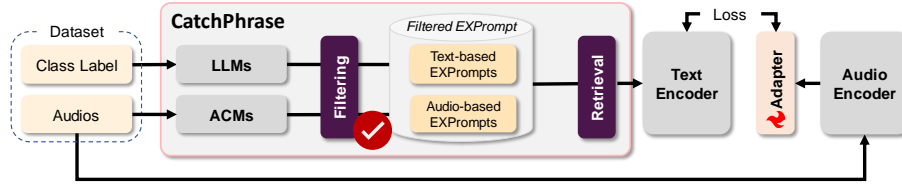
E More on EXPrompt Mining

In this section, we present the exact queries used for EXPrompt construction (see Tab. 10) and instance-based prompts (see Tab. 11) and instance-based EXPrompts (see Tab. 12), corresponding to class-level and instance-level semantics, respectively.

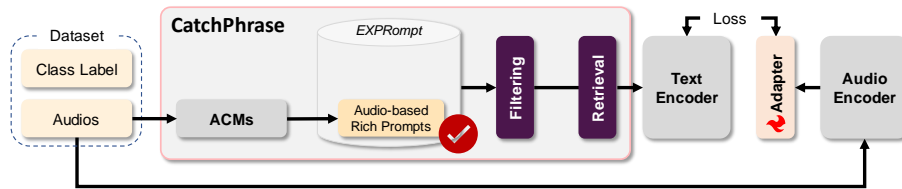
Merge Before Filtering



Merge After Filtering



Audio-only Filtering



Text-only Filtering

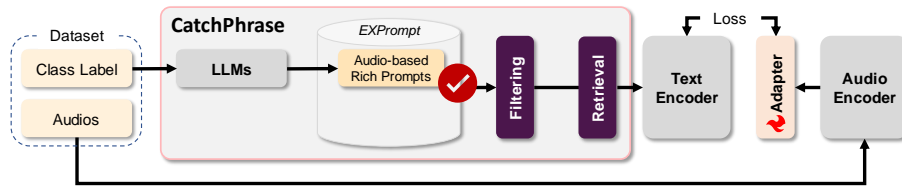


Figure 10: Various component sequences in consisting CatchPhrase.

Table 9: Experiment for CLAP-based filtering parameters. *cls* denotes the abbreviation of class. For US8K and VGGSound, audio subsets of 10, 50, and 100 samples per class were constructed, whereas for ESC-50, subsets of 10, 20, and 30 samples per class were used due to its smaller class size. Performance was measured and compared using the AIS score (higher is better)

| | US8K | | | ESC50 | | | VGGSound | | |
|--------|--------------|--------------|---------|--------|--------------|--------------|----------|--------|--------------|
| | 10/cls | 50/cls | 100/cls | 10/cls | 20/cls | 30/cls | 10/cls | 50/cls | 100/cls |
| Top-1 | .1346 | .1388 | .1400 | .2155 | .2246 | .2304 | .1966 | .1914 | .2004 |
| Top-5 | .1594 | .1724 | .1619 | .1538 | .1513 | .1663 | .1534 | .1665 | .1602 |
| Top-10 | .1630 | .1572 | .1659 | .1389 | .1545 | .1420 | .1453 | .1392 | .1476 |
| Top-20 | .1559 | .1538 | .1648 | .1093 | .1193 | .1229 | .1374 | .1427 | .1384 |
| Top-1 | .1114 | .1091 | .1075 | .1718 | .1763 | .1827 | .1036 | .1127 | .1136 |
| Top-5 | .1380 | .1316 | .1347 | .1934 | .2035 | .1982 | .1288 | .1287 | .1313 |
| Top-10 | .1457 | .1584 | .1511 | .1994 | .1981 | .1847 | .1264 | .1249 | .1235 |
| Top-20 | .1636 | .1574 | .1588 | .1993 | .1815 | .1953 | .1213 | .1277 | .1282 |

Table 10: Set of queries employed for EXPrompt generation, conditioned on class labels. Visual, Auditory, and Semantic queries through large language models. The bolded words represent the key terms in each query.

| Category | Queries |
|----------|---|
| Visual | Describe what a(n) ___ looks like in real world. |
| | What does a(n) ___ looks like in real world? |
| | Describe an image from the internet of a(n) ___ looks in real world. |
| Audio | Describe what a(n) ___ sounds like in real world. |
| | What does a(n) ___ sound like in real world? |
| | Describe a sound from the internet of a(n) ___ in real world. |
| Semantic | Create one sentence about meaning of a(n) ___ in real world: |
| | Summarize a(n) ___ in a single sentence. |
| | Describe what a(n) ___ represents in a real-world context in one sentence. |

Table 11: Example of class-based EXPrompt. Representative EXPrompts generated by processing weak class labels with visual, auditory, and semantic queries through large language models. The bolded words indicate either information related to other classes or the presence of homographs within each EXPrompt.

| Class | Generated Rich Prompts |
|----------|---|
| Crickets | A cricket is a small insect that typically measures around inch in length It has a round and flattened body. |
| | Crickets are small, insectivorous insects that are commonly found in grassy areas. |
| | The image shows a close-up of a group of crickets crawling on a patch of green grass. |
| | A cricket’s sound is often described as a high-pitched chirping |
| | In the real world, crickets make a chirping or buzzing sound. |
| Insects | The constant buzzing of wings as tiny insects dart through the air. |
| | The sound of crickets chirping loudly can be heard in the background. |
| | The buzzing symphony of cicadas, crickets , and grasshoppers fill the warm summer air. |
| | The buzzing of a thousand tiny wings fills the air. |
| | An insect buzzing. |
| Siren | A siren is a type of loud noise-making device used for emergency purposes. |
| | A mythological creature with the upper body of a beautiful woman and the lower body of a bird or fish. |
| | A beautiful, ethereal siren perched on a rocky outcrop overlooking the ocean. |
| | A siren in the real world sounds like a loud, high-pitched wailing noise. |
| | A siren is a loud warning device used to alert people of impending danger. |

Table 12: Example of instance-based EXPrompt. Representative EXPrompts generated by audio instance through ACMs. The bolded words indicate the presence of information related to other classes within each EXPrompt.

| Class | EXPrompts |
|----------|---|
| Crickets | Wind blows and birds chirp in the distance. |
| | Crickets chirp and frogs croak . |
| | A small motor is running and rattling . |
| | Frogs croaking and birds chirping . |
| | Crickets chirp in the distance. |
| Insects | A man speaking followed by rustling and buzzing |
| | Crickets chirp and insects buzz. |
| | Insects buzzing and birds chirping . |
| | Birds are chirping and insects are buzzing. |
| | Insects are buzzing and birds are chirping . |
| Siren | An emergency siren is triggered and passes by. |
| | An emergency siren is triggered and moves closer. |
| | An emergency siren is triggered and moves closer. |
| | An emergency siren is triggered and a horn is triggered. |
| | An emergency siren is triggered while people talk in the background. |



Figure 11: Differences in generated images based on the top-K parameter in the filtering method. A counter effect is observed during filtering: as the value of top-K decreases, the diversity of the generated images also decreases.

Table 13: Audio to Text retrieval results. The retrieval results are reported in terms of R@1.

| Method | US8K | ESC50 | VGGSound |
|--------------|--------------|--------------|--------------|
| GlueGen [35] | 11.3% | 25.5% | 10.4% |
| CatchPhrase | 88.7% | 74.5% | 89.6% |

F Audio to Text Retrieval

To evaluate whether EXPrompt is truly related to the audio, we compared it against the predefined template-based prompts used in the original GlueGen. Specifically, we measured whether the prompt with the highest retrieval top-1 similarity to the test set audio samples originated from EXPrompt or from the baseline prompts. For this evaluation, we employed CLAP as the text and audio encoder. The results show that the proposed EXPrompt achieves higher audio-to-text retrieval performance compared to the baseline method, indicating that our approach constructs text representations that are more closely aligned with the audio content.

G User Studies

A total of 30 participants were asked to compare 15 pairs of images generated from audio inputs using GlueGen and CatchPhrase. Participants responded to two questions: (1) “Which image is most relevant to the given audio?” to evaluate the perceptual alignment between the audio and the generated images, and (2) “Which image is most relevant to the given audio and its associated text?” to assess whether additional textual information helps mitigate auditory illusion effects. As shown in Tab. 14 suggest that CatchPhrase more effectively aligns audio and image semantics, especially in cases where textual context is required to resolve ambiguity. This supports the claim that our method successfully incorporates enriched prompts to improve cross-modal understanding.

Table 14: User studies results. (1), (2) denote the questions asked to participants.

| Method | (1) | (2) |
|--------------|---------------|---------------|
| GlueGen [35] | 35.78% | 19.78% |
| CatchPhrase | 64.22% | 80.22% |

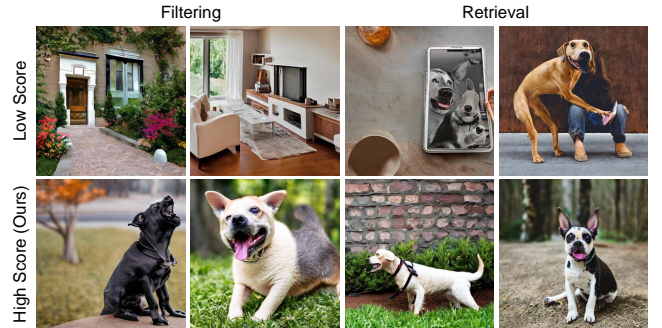


Figure 12: Qualitative results for low- vs. high-scoring EXPrompts in filtering and retrieval. The audio samples used in this experiment are dog bark recordings from the US8K dataset. The top row shows images generated after training with low-scoring prompts, while the bottom row shows results using high-scoring EXPrompts selected by our proposed method. Since the scoring is applied at both the filtering and retrieval stages, we present comparisons for each component.

H Qualitative Results for EXPrompt Scoring

We applied the proposed scoring method across both filtering and retrieval components. While the individual contributions of each component were validated through ablation studies, we additionally examined qualitative results to assess how high- versus low-scoring EXPrompts affect the generated images. As shown in Fig. 12, high-scoring prompts lead to images that are semantically aligned with the corresponding audio, whereas low-scoring prompts tend to produce visually plausible but semantically mismatched outputs. This observation underscores the effectiveness of our scoring and selection strategy.

Notably, in the filtering stage, the presence of noisy prompts generated by LLMs and ACMs causes low-scoring EXPrompts to yield largely random images. In the retrieval stage, although the EXPrompts have already been filtered once, using low-scoring prompts still results in images that reflect only the dominant class information (e.g., “dog”) from the audio, failing to capture finer details such as the sub-concept “bark” and degrading overall image quality. By contrast, our approach—applying high-scoring EXPrompts in both filtering and retrieval—successfully preserves the semantic content of the audio and enhances the fidelity of the generated images.

I Limitation

Despite the promising results, our study has several limitations that warrant further investigation. First, due to the limited information available in the training data, zero-shot audio-to-image generation remains an open and challenging problem that has yet

to be thoroughly explored. Second, generating images from audio with multiple overlapping events continues to pose significant challenges, as disentangling and accurately representing such complex

auditory scenes is inherently difficult. Lastly, incorporating temporal segmentation could potentially improve the model's ability to handle sequential events in audio. Addressing these challenges constitute an important direction for future research.